

# Dynamics of electric-field-induced molecular reorientation of a surface-stabilized antiferroelectric liquid crystal in the smectic- $C^*$ phase probed by time-resolved infrared spectroscopy

A. L. Verma,<sup>1,\*</sup> B. Zhao,<sup>2</sup> A. Bhattacharjee,<sup>1</sup> and Y. Ozaki<sup>3,\*</sup><sup>1</sup>*Department of Physics, North-Eastern Hill University, Shillong 793022, India*<sup>2</sup>*Key Laboratory of Supramolecular Structure and Spectroscopy, Jilin University, Changchun, 130023, People's Republic of China*<sup>3</sup>*School of Science, Kwansai-Gakuin University, Ueghara, Nishinomiya 662-8501, Japan*

(Received 2 August 2000; published 19 April 2001)

Polarization dependent and time-resolved Fourier transform infrared studies have been carried out on the electric-field-induced ferroelectric phase (Sm- $C^*$ ) of a chiral, antiferroelectric liquid crystal at different temperatures. Polarization dependent infrared spectra under dc electric field reveal that the average alkyl chain axis does not coincide with the mesogen axis and is less tilted with respect to the layer normal than the mesogen. The analysis of the various absorbance profiles obtained from temporal response of absorption changes of infrared bands at different time delays provides clear evidence for biased orientation and hindered rotation of almost all the molecular segments around the average molecular long axis and the rotation of the whole molecule around its axis is also hindered. It is further inferred that the mesogen, the chiral segment, and the alkyl chains reach their equilibrium orientations at nearly the same time on switching the polarity of the ac electric field but the different molecular segments reorient through different angles.

DOI: 10.1103/PhysRevE.63.051704

PACS number(s): 61.30.-v

## I. INTRODUCTION

Chiral ferroelectric liquid crystals (FLC) belong to an important class of compounds because of their potential applications in the fast electro-optic devices, high-resolution printheads, flat panel displays, and many other fields [1–4]. Generally, the molecules forming the liquid-crystalline phases have a number of conformational and orientational states and their statistical distribution and equilibrium populations strongly influence the physical and electro-optical properties [5–6]. The conformation and orientation of the alkyl chains with respect to the average long molecular axis, flexibility of the core and hindered rotation of the molecular segments like carbonyl groups located near the chiral carbon are expected to play a dominant role in influencing the dynamical behavior of the system.

In recent years, time-resolved Fourier transform infrared (FTIR) spectroscopy has been one of the most extensively employed and powerful techniques for probing the switching dynamics of different molecular segments in liquid crystals [7–16]. By this technique, one can probe the mobility and switching behavior of each segment of a liquid-crystal molecule separately as infrared spectroscopy has the advantage of being bond specific. Two broad ideas have emerged from previous studies. Some believe that the whole molecule behaves as a rigid unit and all the molecular segments reorient nearly simultaneously [5–10] whereas others have shown that the different molecular segments respond and reorient at different times [11–16]. However, the switching dynamics of ferroelectric liquid crystals at molecular segmental level is a very complicated process and many basic aspects of dynamical behavior of FLC's have yet to be clarified.

As a part of our continuing efforts [12–16] to explore the

mechanism of electric-field induced reorientation of different segments of the surface stabilized ferroelectric liquid crystals in the Sm- $C^*$  phase, we report in this paper a time-resolved FTIR study on a chiral, antiferroelectric liquid crystal (Chisso-2061) to monitor the response of different molecular segments under pulsed electric field. From detailed analysis of the temporal responses of absorption changes of selected IR bands over a range of polarizer orientations, we have found clear evidence for hindered rotation of all the molecular segments around the long molecular axis. It is also inferred that both the mesogen and alkyl chains start reorienting immediately on application of the electric field, and that the mesogen as well as the alkyl side chains reorient at almost the same rate during the process of electro-optical switching. In contrast to previous results [5–16], our studies also indicate that the rotation of the whole molecule is not free but is biased around the long molecular axis.

## II. EXPERIMENTAL DETAILS

Chiral AFLC, 4-(1-methylheptyloxy carbonyl) phenyl 4-(4'-octyloxy benzoyloxy) benzoate, named as Chisso 2061, was obtained from the Chisso Company, Japan. The structure and the phase-transition sequence (Fig. 1) of the sample are shown in Fig. 1.

The details of the sample cell are the same as reported in our earlier work [13]. Monodomains of the sample inside the cell were obtained by employing cyclic and slow tempera-

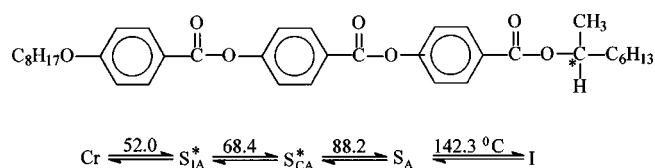


FIG. 1. Structure of the Chisso-2061 chiral antiferroelectric liquid crystal and its phase-transition temperatures.

\*Authors to whom correspondence should be addressed.

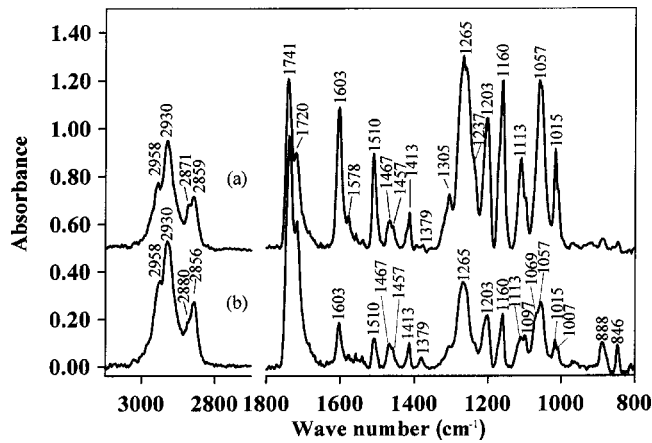


FIG. 2. Polarized FT-IR spectra of Chisso 2061 at 75 °C in the (a) parallel and (b) perpendicular polarization geometries. Resolution,  $4 \text{ cm}^{-1}$ , 100 accumulations.

ture treatment under an electric field of  $\pm 15 \text{ V}$ . A JOEL JIR-6500 FTIR spectrometer equipped with a microattachment (JEOL IR-MAU 110) and a mercury-cadmium-telluride detector was used for obtaining the data. A wire grid polarizer was rotated about the direction of the IR radiation. The polarization direction was fixed at  $45^\circ$  to the

rubbing direction. In order to make time-resolved measurements the same instrument equipped with a boxcar integrator (SRS Model 250) was used. Rectangular wave electric field of  $\pm 15 \text{ V}$  at  $5 \text{ kHz}$  repetition rate was applied between the electrodes of the cell from a function generator (Kenwood FG-273). The time-resolved polarized spectra were measured from 0 to  $100 \mu\text{s}$  with a resolution of  $4 \text{ cm}^{-1}$  and 100 scans were accumulated in each case. Baseline corrections of the spectra were made using a nonlinear spline function and curve fitting was done using GRAMS software. As the different spectral regions show many overlapping components, we have deconvoluted the relevant bands and have used the peak heights of the deconvoluted components as a measure of absorbance.

### III. RESULTS AND DISCUSSION

Figure 2 shows polarized IR spectra as a function of the polarization angle  $\omega$  for a monodomain of the sample in the  $\text{Sm-C}_A^*$  phase at  $\omega = 0^\circ$  and  $90^\circ$ . The polarization angle  $\omega$  is the angle between the direction of rubbing (i.e., the smectic layer normal) and the polarization direction of the incident IR radiation; and is taken to be zero when these two directions coincide. From these spectra the dichroic ratio  $D$ , defined as the ratio of absorbances for the parallel and perpen-

TABLE I. Dichroic ratio ( $D$ ) and vibrational band assignment for the relevant peaks in the infrared spectra of Chisso-2061 liquid crystal in the  $\text{Sm-C}_A^*$  phase at 75 °C.

Wave number ( $\text{cm}^{-1}$ )	$D(A_{\parallel}/A_{\perp})$	Assignment
2958	1.17	$\text{CH}_3$ asym st.
2930	0.50	$\text{CH}_2$ antisym st.
2871	1.17	$\text{CH}_3$ sym st.
2859	0.85	$\text{CH}_2$ sym st.
1741	0.57	$\text{C}=\text{O}$ st. (Ph-COO-Ph) (core)
1720	0.66	$\text{C}=\text{O}$ st. (Ph-COO-R) (chiral)
1603	7.66	$\text{C}=\text{C}$ (phenyl) st.
1578	2.70	$\text{C}=\text{C}$ (phenyl) st.
1510	3.36	$\text{C}=\text{C}$ (phenyl) st.
1504	3.42	$\text{C}=\text{C}$ (phenyl) st.
1467	1.07	$\text{CH}_2$ scissoring mode
1457	0.81	$\text{CH}_2$ scissoring mode
1421	2.08	$\text{CH}_2$ scissoring mode
1413	2.06	$\text{CH}_2$ scissoring mode
1379	0.10	$\text{CH}_3$ in-plane deformation
1324	1.67	Phenyl $\text{C}=\text{C}$ in plane
1305	5.67	Phenyl $\text{C}=\text{C}$ in plane
1265	4.11	$\text{C}-\text{O}$ st.
1237	4.63	$\text{C}-\text{O}$ st.
1203	4.58	$\text{C}-\text{O}$ st. ?
1160	7.32	Phenyl $\text{C}-\text{H}$ in plane deformation
1113	2.37	$\text{C}-\text{C}-\text{C}$ in plane stretch and $\text{CH}_3$ rock
1097		Phenyl $\text{C}-\text{H}$ in plane deformation
1057	4.28	Phenyl $\text{C}-\text{H}$ in plane deformation
1015	6.67	Phenyl $\text{C}-\text{H}$ in plane deformation
888	0.12	$\text{C}-\text{C}-\text{C}$ in plane stretch and $\text{CH}_3$ rock
846	0.37	Skeleton

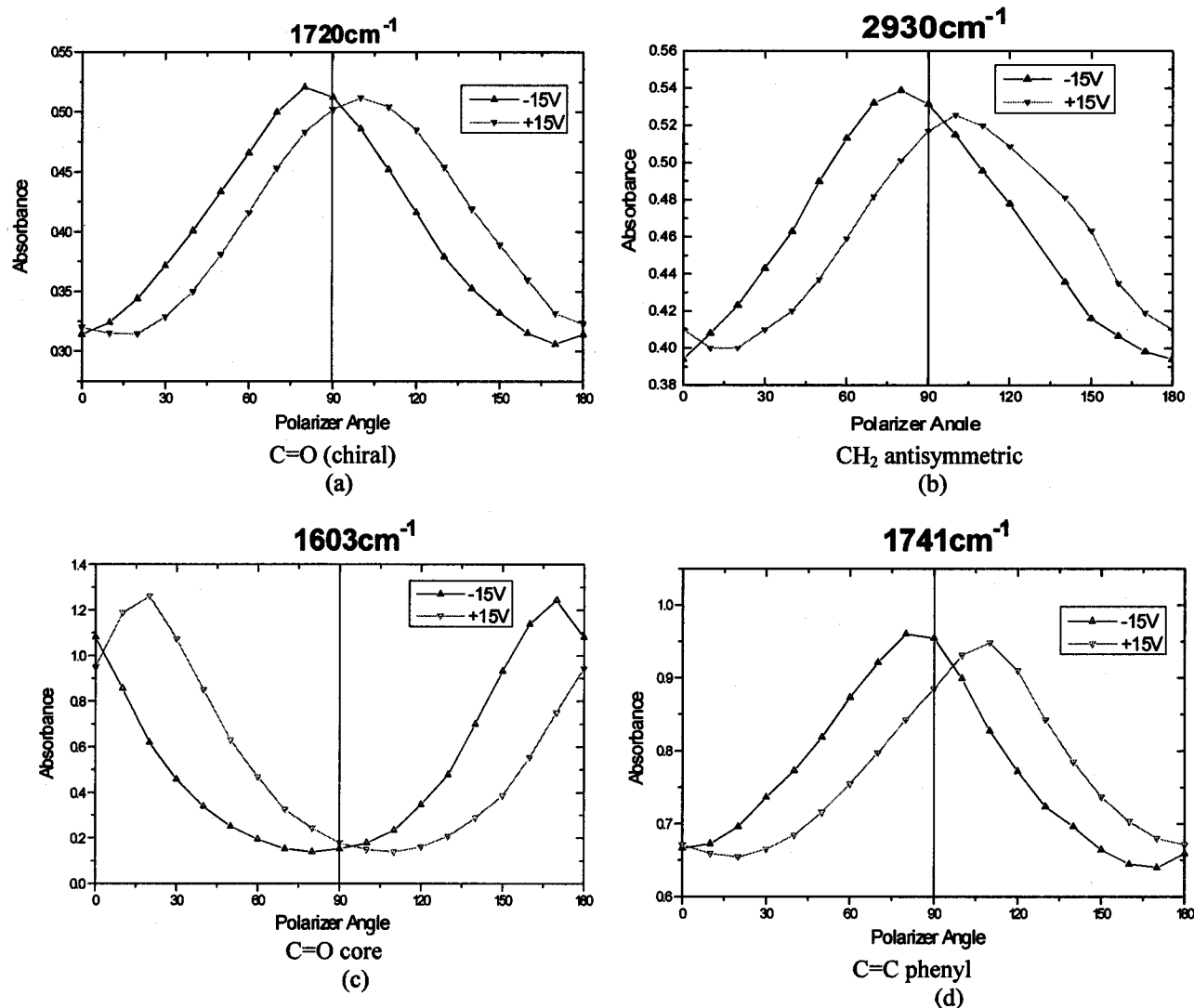


FIG. 3. Plots representing the absorbance (arbitrary units) as a function of polarizer angles  $\omega$  at 75 °C for the various segments of Chisso-2061 in the Sm-C\* phase on application of  $\pm 15$  V dc electric field.

dicular polarizations of light, were calculated for different bands. Table I lists the assignment of the bands based on expected group frequency considerations and previous works [18–20] with their dichroic ratios. It is to be noted that due to the presence of  $-\text{CH}_2$  and  $-\text{CH}_3$  groups in both the achiral and the chiral chains, only averaged information can be obtained from the C–H stretching modes. A noticeable feature observed is that the dichroic ratios for the alkyl chain modes are  $\leq 1$ , which can be ascribed to the disorder of the chains. For the bands related to the mesogen segments, the dichroic ratio is found to vary widely ( $\approx 2.3$  to 7.6) suggesting that there is substantial disorder in the core and also that the benzene rings may be skewed with respect to each other in the Sm-C<sub>A</sub>\* phase. An interesting feature in the IR spectrum is the observation of two components in the C=O stretching mode region at 1741 and 1720  $\text{cm}^{-1}$ . The origin of the former is attributed to the C=O groups between the phenyl rings and that of the latter is ascribed to the C=O groups adjacent to the chiral part.

For detailed study on the behavior of different molecular

segments, few relevant and comparatively isolated bands were chosen. The band at 2930  $\text{cm}^{-1}$  ( $\text{CH}_2$  antisymmetric stretch) provides information that is exclusive to the alkyl chain portion. The bands observed at 1741 ( $\nu_{\text{C=O}}$ ), 1510 ( $\nu_{\text{C=O}}$ ), 1603 ( $\nu_{\text{C=O}}$ ), and 1160  $\text{cm}^{-1}$  (phenyl ring C–H in plane deformation) are all related to the mesogen portion while one clear band at 1720 ( $\nu_{\text{C=O}}$ )  $\text{cm}^{-1}$  is related to the chiral portion of the molecule. At zero applied voltage the mesogen bands show parallel dichroism with their maximum intensity ( $I_{\text{max}}$ ) at  $\omega = 0^\circ$  and  $180^\circ$  while the alkyl chain bands exhibit perpendicular dichroism with their  $I_{\text{max}}$  at  $\omega = 90^\circ$  and  $270^\circ$ . For monitoring the relative orientation of the alkyl chain, mesogen, and the chiral segments, polarization-dependent IR spectra of the sample in the electric-field induced Sm-C\* phase were measured at 75 °C under dc voltages of 0 and  $\pm 15$  V. The polarization dependence of absorption peaks can be conveniently described by the plots in Fig. 3 where the peak absorbance  $A(\omega)$  at a particular polarization angle  $\omega$  is plotted as a function of  $\omega$ . It is clear from this figure that the absorbance of the bands

TABLE II. Values of angular shift  $\omega$  of peak profiles and total angular variation  $\Delta\omega$  with applied electric field in the Sm-C\* phase of Chisso-2061 at 75 °C.

Bank position $\Rightarrow$	1160 $\text{cm}^{-1}$	1203 $\text{cm}^{-1}$	1510 $\text{cm}^{-1}$	1602 $\text{cm}^{-1}$	1720 $\text{cm}^{-1}$	1741 $\text{cm}^{-1}$	2930 $\text{cm}^{-1}$
-15 V	10°	7°	10°	10°	7°	10°	9°
15 V	-18°	-14°	-18°	-18°	-14°	-18°	-14°
$\Delta\omega$	28°	21°	28°	28°	21°	28°	23°

for all the three segments attain their maxima at different angles of polarization. Another very interesting observation in this study is that the absorbances for the bands associated with the different segments maximize at different angles for negative and positive bias voltages. For example, the mesogen bands at 1510 and 1603  $\text{cm}^{-1}$  at 75 °C show absorbance maxima at  $\omega = -18^\circ$  at +15 V whereas the absorbance maxima occurs at  $\omega = +10^\circ$  at -15 V. Similar variations in the angular shifts of the peak profiles for the bands associated with the other segments of the molecule have been observed, the details of which are given in Table II. Also one can see that the observed rotation of the absorbance maxima for positive and negative polarity  $\Delta\omega$  is distinctly different for the bands related to the different segments. The maximum tilt angle  $\Delta\omega$  for the bands due to the mesogen is 28°, that for the alkyl chains is 23° whereas for the modes related to the chiral part it is 21°. As the estimated uncertainty in the measurement of the polarization angles is not more than  $\pm 1^\circ$ , these differences in the value of  $\omega$  for positive and negative biasing are very significant. Qualitatively, one can understand the different values of the maximal tilt angles  $\Delta\omega$  for the mesogen and alkyl chains modes in terms of a steric and zigzag model of the molecules arranged in smectic layers where the aromatic cores may be packed up in a higher tilted orientation in the smectic layers than the molecule as a whole. On the other hand, the inconsistency in the angular shifts in the peak positions for the positive and negative polarity of the applied electric field provides strong evidence that the rotation of the molecule along the long molecular axis is not free and is a clear manifestation of the hindered rotation. In other words, it appears that the rotation of the whole molecule is biased around its long molecular axis with the molecule adopting some preferential orientation. This important finding is also supported by our time-resolved studies (see later). Although the interface-induced electroclinic effect may play some role for the observed inconsistencies in the orientations of different segments of the molecule, this effect alone cannot explain the different values of maximal tilt angles  $\Delta\omega$  for the mesogen and alkyl chains modes and other effects observed during dynamical switching.

In order to understand the behavior of the system in details, we consider a vibrational mode  $N$  of the molecule confined in a laboratory frame of reference with its transition dipole moment  $\mathbf{p}$  oriented along a fixed angle  $\alpha_N$  with respect to the molecular axis  $M$ . The molecular axis  $M$  is, in turn, oriented with respect to the mean orientation direction  $\mathbf{n}$  by an angle  $\theta$ .

Then the long axis order parameter about  $\mathbf{n}$  is given by [19]

$$S = \langle P_2(\cos \theta) \rangle = 1/2 \langle (3 \cos^2 \theta - 1) \rangle, \quad (1)$$

where  $P_2$  is a Legendre polynomial of order 2. The dichroic ratio is related to the average  $\langle \cos^2 \theta \rangle$  for a particular band whose transition dipole moment is oriented at an angle  $\alpha_N$  relative to the long molecular axis by the relation [21]

$$\begin{aligned} D(S, \alpha_N) &= A_Z/A_Y = [1 + 2P_2(\cos \alpha_N)S] / [1 - 2P_2(\cos \alpha_N)S] \\ &= \{ \frac{1}{2} \sin^2 \alpha_N \cos^2 \theta [1 - \langle (\cos^2 \theta) \rangle S] + \cos^2 \theta \langle \cos^2 \alpha_N \rangle \} / \{ \frac{1}{2} \sin^2 \alpha_N \cos^2 \theta [1 - \langle (\cos^2 \theta) \rangle S] + \cos^2 \theta \langle \cos^2 \alpha_N \rangle \}. \end{aligned} \quad (2)$$

The mean orientation of the transition dipole moment with respect to the average long molecular axis is obtained as

$$\cos^2 \alpha_N = 1/3 [2(D-1)/S(D+2) + 1]. \quad (3)$$

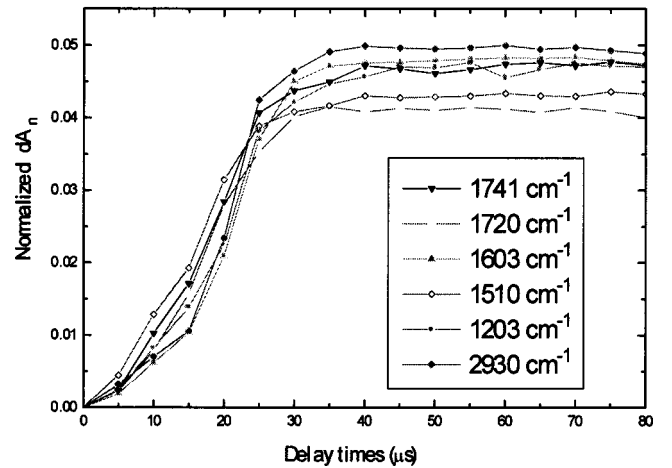


FIG. 4. Time dependence of the normalized intensity changes  $dA_n$  vs the delay time for the representative IR bands for the chiral, the alkyl chains, and the mesogen segments of Chisso-2061 molecule at 75 °C on application of square-wave electric field of the  $\pm 15$  V and 5 kHz repetition rate.

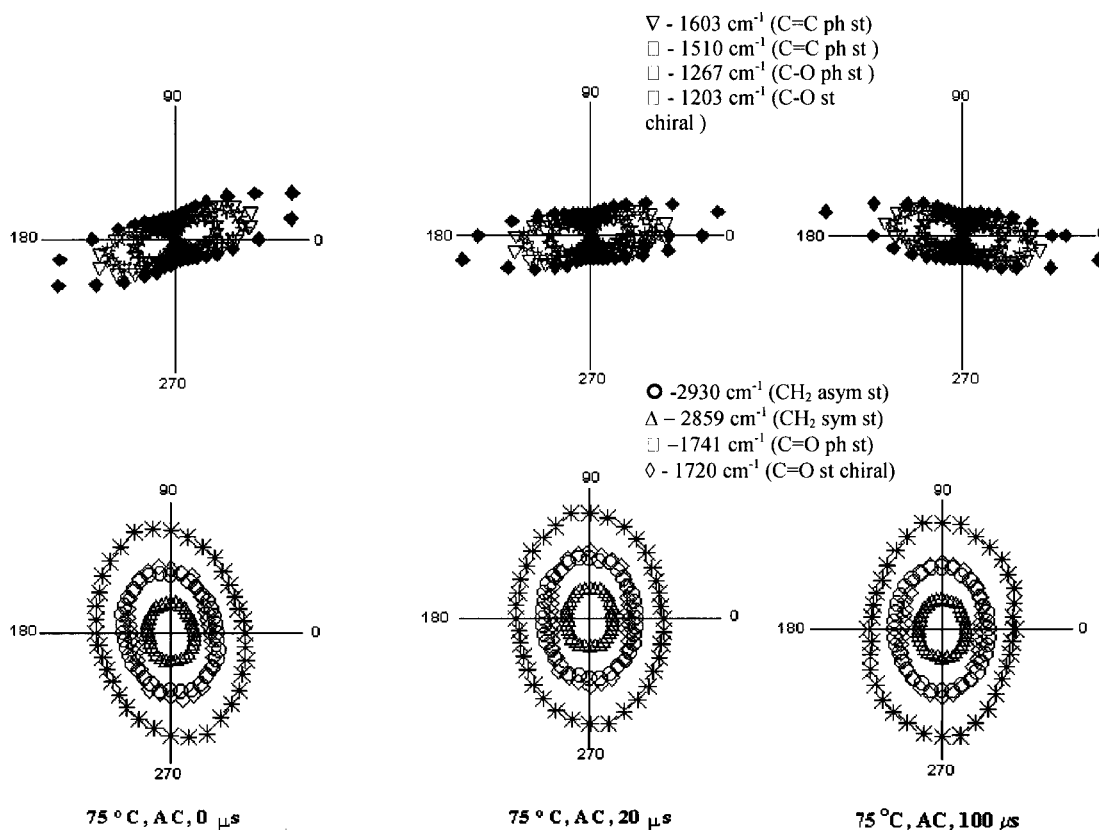


FIG. 5. Polar plots of the peak absorbance  $A(\omega)$  vs the polarization angle  $\omega$  before and during the dynamical switching of the Chisso-2061 in the  $\text{Sm-C}_A^*$  phase at 0, 20, and 100  $\mu\text{s}$  at 75  $^\circ\text{C}$  and applied voltage pulse of  $\pm 15$  V and 5 kHz repetition rate for the selected bands characterizing the alkyl chains, mesogen, and the chiral segments.

As the value of the dichroic ratio for the C-O stretches observed at 1265 and 1237  $\text{cm}^{-1}$  are relatively large ( $>4$ ), therefore we can assume that the transition dipole moment for these bands lie along the long molecular axis, i.e.,  $\theta=0$  in these cases. Using this in Eq. (1) we obtain the value of  $S$  to be 0.92. This value of  $S$  along with the value of  $D$  measured from our experiments is used to calculate the mean orientation  $\alpha_N$  of the transition dipole moments. The average values of  $\alpha_N$  are obtained as 24 $^\circ$ , 36 $^\circ$ , 24 $^\circ$ , 61 $^\circ$ , 62 $^\circ$ , and 64 $^\circ$  for the bands observed at 1160, 1510, 1603, 1720, 1741, and 2930  $\text{cm}^{-1}$ , respectively. These values of  $\alpha_N$  indicate that the deviations from isotropic averaging of different functional groups, about the long molecular axis, are not negligible.

As stated earlier we have found that the dichroic ratio of the C=C stretching modes at 1603  $\text{cm}^{-1}$  is 7.66 while for the other phenyl ring modes it varies from 2.7 to 7.3. A magnified view of the spectrum shows the presence of fine structures in the bands that may originate from the combined effects of nonplanarity of the benzene rings having different environments and conformational isomers of the core. In similar types of compounds, the *para*-benzene ring axis is found to be tilted from the long molecular axis by more than 20 $^\circ$  [20–22]. The torsional angle  $\angle \text{C}_{\text{C=O}}-\text{O}-\text{C}_{\text{Ph}}-\text{C}_{\text{Ph}}$  is reported to be around 55 $^\circ$  whereas the torsional angle  $\angle \text{C}_{\text{Ph}}-\text{C}_{\text{Ph}}-\text{C}_h-\text{O}$  is only about 5 $^\circ$ . Hence the core of the

molecule is nonplanar with the benzene rings skewed with respect to each other by about 50 $^\circ$  to 60 $^\circ$ . Similar results have also been obtained using quantum orbital calculations on related molecules [20,23,24]. Due to the nonplanar structure and hindered rotation of the molecule around its long molecular axis, it will not reorient to mirror symmetric position on changing the polarity of the electric field. The electrostatic and quadrupolar interactions between the chiral center and the nonsymmetrically distributed highly polarizable groups, such as carbonyl groups, are likely to contribute significantly to the molecular anchoring strength, which will influence the rotational freedom of the molecules. As a result of these interactions, the molecule may not reorient freely with change in the electric field bias but may adopt some privileged orientation.

On the basis of these findings it is inferred that in the Chisso-2061 sample in the  $\text{Sm-C}_A^*$  phase, the alkyl chains are tilted at a different angle with respect to the smectic layer normal in the equilibrium state. In this static arrangement the magnitude of the tilt angle for the various segments depends on the polarity of the applied voltage. There is a substantial disorder in the alkyl chains due to the presence of gauche conformations. The benzene rings are also skewed with respect to each other. When the polarity is reversed, the applied electric field rotates the different segments of the molecule to new positions, which are not mirror symmetric about the layer normal.



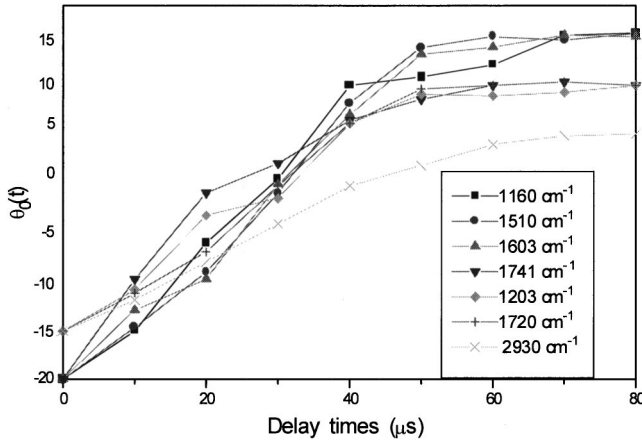


FIG. 6. Time dependence of the mean orientation angle  $\theta_0(t)$  as a function of delay time for the representative bands of Chisso-2061, at 75 °C on application of square-wave electric field of  $\pm 15$  V and 5 kHz frequency.

#### IV. DYNAMICAL SWITCHING BEHAVIOR

In order to probe the dynamical switching behavior from one surface stabilized state to another on application of ac electric field, time-resolved infrared measurements were carried out. FTIR spectra of the sample were recorded at 75 °C on application of  $\pm 15$  V at a 5 kHz repetition rate. The participation of all the segments in the switching process is evident from the intensity variations of the associated modes on the change of polarity of the electric field. As the tilt angle varies with the applied electric field and temperature, the normalized absorbance changes  $dA_n$  were calculated for a quantitative comparison of the reorientation rates of molecular segments at different voltages using the relation

$$dA_n = |A(t) - A(2)| / |A(1) - A(2)|, \quad (4)$$

where  $A(t)$  is the peak absorbance at time  $t$ ,  $A(1)$  and  $A(2)$  are the peak absorbance values at the surface stabilized states I (before the application of electric field) and II (when the reorientation is completed), respectively. These plots also provide information about fractional reorientation of the segments of the molecule at a particular time. Figure 4 shows the plot of  $dA_n$  vs delay time during the course of switching for selected bands characterizing the mesogen, chiral, and alkyl chain segments at 75 °C and 15 V amplitude of the voltage pulse. This figure makes it clear that the reorientation from one state towards other state starts immediately on application of the field and the normalized absorbances of the various modes show a very similar rate of increase till a saturation point is attained. After a certain period ( $\approx 28 \mu\text{s}$ ), the molecule attains the second surface-stabilized state. A significant point to be noted here is that all the segments of the molecule appear to switch (i.e., attain the second surface

stabilized state) at the same time under the present experimental conditions. To quantify the field induced orientations on application of an ac electric field, measurements conducted before, during, and after the switching process, reveal beyond uncertainty limits that the magnitudes of orientation angles of the peak absorbances of the different bands are not equal as shown in Fig. 5. For example, change in  $\omega$  for the mesogen bands at 1603 and 1510  $\text{cm}^{-1}$  is  $-18^\circ$  at 0  $\mu\text{s}$  while it is  $+10^\circ$  at 80  $\mu\text{s}$ . The net change in the orientation of the dipole moment for the core bands is  $28^\circ$  while that for the alkyl chain bands is  $23^\circ$ . The variation in case of the chiral mode was found to be  $21^\circ$ . This trend is consistent with our static data.

For exploring the response of the different molecular segments to the applied ac electric field, we measured the temporal responses of absorbance changes of the representative bands over a range of polarizer orientation at different time delays at 10  $\mu\text{s}$  time intervals. In Fig. 6 we have plotted mean orientation angle  $\theta_0(t)$  as a function of delay time for the representative bands of different segments. A significant feature seen here is that the different segments reorient through different angles. The modes related to the mesogen reorient from  $-20^\circ$  to  $+15^\circ$ , those related to the chiral part reorient from  $-15^\circ$  to  $+10^\circ$ , whereas the alkyl chain modes switch from  $-15^\circ$  to  $+5^\circ$ . This figure also shows that there is no induction period for any segment of the molecule within the present experimental conditions. These results are fully consistent with our static data under dc electric field. The nonisotropic rotation of the molecule along its long molecular axis is manifested in the dynamic switching as well as in experiments done under dc electric field. We suggest that the inconsistency in the angular shifts in the peak positions arises as a result of anisotropic interactions among the noncylindrically distributed dipoles leading to the formation of nonsymmetric surface stabilized states where the average molecular axis may align along two directions at different angles from the normal to the smectic layers.

To conclude, this paper demonstrates that contrary to the existing beliefs, not only the individual segments but the reorientation of the entire molecule along the long molecular axis is biased in this FLC. It is also observed that the different segments reorient through different angles during dynamic switching as well as under dc electric field. The benzene rings are found to be skewed with respect to each other forming a nonplanar structure, which results in a distorted packing of the aromatic cores in the smectic layers.

#### ACKNOWLEDGMENTS

The major part of the experimental work was done when A.L.V. and B.Z. were staying at the Kwansai Gakuin University, Nishinomiya, Japan as visiting professors. A.L. V and A.B. are grateful to DST, New Delhi for financial assistance. The authors are grateful to Dr. S. Saito of Chisso Petrochemical corporation, Japan for providing the Chisso-2061 sample.

- [1] S. T. Lagerwell, N. A. Clark, J. Dijon, and J. F. Clerc, *Ferroelectrics* **94**, 30 (1989).
- [2] N. A. Clark, and S. T. Lagerwell, *Appl. Phys. Lett.* **36**, 899 (1980).
- [3] S. Matsumoto, A. Maruyama, H. Hatho, Y. Kinoshita, H. Harai, M. Ishikawa, and S. Kamagani, *Ferroelectrics* **85**, 235 (1988).
- [4] J. Dijon, in *Liquid Crystals, Application and Uses*, edited by B. Bahadur (World Scientific, Singapore, 1990), Vol. 1, p. 305.
- [5] K. H. Kim, K. Ishikawa, H. Takezoe, and A. Fukuda, *Phys. Rev. E* **51**, 2166 (1995).
- [6] B. Jin, Z. Ling, Y. Takanishi, K. Ishikawa, H. Takezoe, A. Fukuda, M. Kakimoto, and T. Kitazume, *Phys. Rev. E* **53**, R4295 (1996).
- [7] N. Katayama, M. A. Czarnecki, M. Satoh, T. Watanabe, and Y. Ozaki, *Appl. Spectrosc.* **51**, 487 (1997).
- [8] S. V. Shilov, H. Skupin, F. Kremer, E. Gebhard, and R. Zentle, *Liq. Cryst.* **22**, 203 (1997).
- [9] S. V. Shilov, S. Okretic, H. W. Siesler, and M. A. Czarnecki, *Appl. Spectrosc. Rev.* **31**, 82 (1996).
- [10] S. V. Shilov, H. Skupin, F. Kremer, T. Wittig, and R. Zentle, *Phys. Rev. Lett.* **79**, 1686 (1997).
- [11] F. Hide, N. A. Clark, K. Nito, A. Yasuda, and D. M. Walba, *Phys. Rev. Lett.* **75**, 2344 (1995).
- [12] A. L. Verma, B. Zhao, H. Terauchi, and Y. Ozaki, *Phys. Rev. E* **59**, 1868 (1999).
- [13] A. L. Verma, B. Zhao, S. M. Ziang, J. C. Shen, and Y. Ozaki, *Phys. Rev. E* **56**, 3053 (1997).
- [14] Y. Nagasaki, K. Masutani, T. Yoshihara, and Y. Ozaki, *J. Phys. Chem.* (to be published).
- [15] Y. Nagasaki, T. Yoshihara, and Y. Ozaki, *J. Phys. Chem.* **104**, 2846 (2000).
- [16] Y. Nagasaki, and Y. Ozaki, *Phys. Chem. Chem. Phys.* (to be published).
- [17] Y. Tian, X. Xu, Y. Zhao, X. Tang, F. Su, X. Zhao, and E. Zhou, *Liq. Cryst.* **19**, 295 (1995).
- [18] J. W. Goodby, R. Blinc, N. A. Clark, S. T. Lagerwell, M. A. Osipov, S. A. Pikin, T. Sakurai, K. Yoshino, and B. Zeks, *Ferroelectric Liquid Crystals: Principles, Properties and Applications* (Gordon and Breach, Philadelphia, 1991).
- [19] J. Michl and E. W. Thulstrup, *Spectroscopy with Polarized Light, Solute Alignment by Photoselection in Polymer, Liquid Crystals and Membranes* (VCH Verlagsgesellschaft, Weinheim, 1986).
- [20] A. Kocot, R. Wzralik, B. Orgasingka, T. Perova, J. K. Vij, and H. T. Nguyen, *Phys. Rev. E* **59**, 551 (1999).
- [21] E. Hild, A. Kocot, J. K. Vij, and R. Zentel, *Liq. Cryst.* **16**, 783 (1994).
- [22] J. K. Vij, A. Kocot, G. Kruk, R. Wrzalik, and R. Zentel, *Mol. Cryst. Liq. Cryst. Sci. Technol., Sect. A* **237**, 337 (1993).
- [23] K. Tishiro, J. Hao, M. Kobayashi, and T. Inone, *J. Am. Chem. Soc.* **112**, 8273 (1990).
- [24] R. Centore and A. Tuzi, *Acta Crystallogr., Sect. C: Cryst. Struct. Commun.* **45**, 107 (1998).